Volume 56
Number 3
11 January 2020
Pages 323–488

ChemComm

Chemical Communications

rsc.li/chemcomm

ISSN 1359-7345

COMMUNICATION

Roland C. Fischer, David J. Liptrot *et al.*

Reductive dehydrocoupling of diphenyltin dihydride with $LiAlH_4$: selective synthesis and structures of the first bicyclo[2.2.1]heptastannane-1,4-diide and bicyclo[2.2.2]octastannane-1,4-diide

ROYAL SOCIETY OF CHEMISTRY

ChemComm

COMMUNICATION

View Article Online
View Journal | View Issue

Cite this: *Chem. Commun.*, 2020, **56**, 336

Received 11th October 2019,
Accepted 28th November 2019

DOI: 10.1039/c9cc07976a

rsc.li/chemcomm

Reductive dehydrocoupling of diphenyltin dihydride with $LiAlH_4$: selective synthesis and structures of the first bicyclo[2.2.1]heptastannane-1,4-diide and bicyclo[2.2.2]octastannane-1,4-diide†

Beate G. Steller, [a] Roland C. Fischer, *[a] Michaela Flock, [a] Michael S. Hill, [b] David J. Liptrot, *[b] Claire L. McMullin, [b] Nasir A. Rajabi,[b] Kathrin Tiefling[a] and Andrew S. S. Wilson [b]

The reaction of diphenyltin dihydride with $LiAlH_4$ gives access to a set of charged tin cages as their lithium salts. Variation in the ratio of reactants provides a perstannabicyclooctane dianion and a perstannanorbornane as the di- and monoanions. These compounds can be synthesised selectively by careful stoichiometric control and have been characterised by single crystal X-ray diffractometry, NMR and UV-vis spectroscopy. Computational exploration of the electronic structures of these compounds was undertaken and, in agreement with structural and spectroscopic features, indicated significant σ-delocalisation in the tin skeletons.

The chemistry of anionic oligo-tin cage and cluster compounds is dominated by a plethora of Zintl phases, discrete Zintl ions,[1] $[Sn_n]^{x-}$, or their derivatisation products, $[R_mSn_n]^{x-}$.[2] Derivatisation reactions of the Zintl ion Sn_9^{4-} have led to the trianionic compounds RSn_9^{3-}.[3] Reaction of thermolabile tin(I) halides with $[Si(SiMe_3)_3]^-$ resulted in the isolation of neutral $Sn_{10}[Si(SiMe_3)_3]_6$,[4] the monoanion $Sn_{10}[Si(SiMe_3)_3]_5^-$,[5] and the dianions $Sn_9[Si(SiMe_3)_3]_4^{2-}$ and $Sn_{10}[Si(SiMe_3)_3]_4^{2-}$.[6,7] Moreover, the anionic cluster $Sn_9R_7(NHC)^-$ (R = $CH(SiMe_3)_2$, NHC = 1,2,3,4-tetramethylimidazol-2-ylidene) was isolated from the reaction of the trihydride $RSnH_3$ with the corresponding NHC.[8] Alongside these, several neutral metalloid clusters of the form Sn_nR_m ($n > m$) have been obtained from reductive or dehydrogenative coupling methods.[9] Closely related to metalloid compounds,[10a] albeit with a superstoichometric ratio of substituents to tin, are the elementoid[10b] [1.1.1]pentastannapropellanes, Sn_5R_6,[11] tetracyclic Sn_7R_8[12] and the hexastannabenzene isomer, Sn_6R_6.[13] The aforementioned compounds share a non-classical, *i.e.* 3D-delocalised, bonding situation. This confers a narrow energy gap between frontier orbitals which facilitates interesting addition chemistry and redox behaviour.[14] In contrast to the well represented class of simple monocyclic rings, $(R_2Sn)_n$,[15] purely σ-bonded tin cages, $(RSn)_n$, are sparse. Examples include tricyclo- and pentacycloprismanes of the stoichiometry, R_6Sn_6 and $R_{10}Sn_{10}$,[8,16] cubanes, R_8Sn_8,[17] and a tetrahedral cage molecule with edge-bridging methandiyl substituents.[18] Anionic, covalent, oligotin cages include $Sn_8R_6^{2-}$ (R = Si-*t*-Bu_3)[16c] and $Sn_5(CH_3)R_6^-$ and the radical anion $Sn_5R_6^-$ (R = 2,6-Et_2-C_6H_3). The latter species originate from the addition of methyl lithium to, and the electrochemical one-electron reduction of, a [1.1.1]pentastannapropellane.[14b] Organotindihydrides are common starting materials in the synthesis of oligotin compounds. Their dehydrogenative coupling has also been widely applied in the synthesis of linear tin polymers and cyclic oligomers $(R_2Sn)_n$,[19] whilst the reaction of a tin dihydride with sodium in liquid ammonia led to the formation of Ph_2SnHNa and $NaPh_2SnSnPh_2Na$.[20]

Diphenyltin dihydride can be synthesised by the reaction of $LiAlH_4$ with diphenyltin dichloride.[21] During our repetition of this literature method, we noted the reaction mixture would often acquire a deep red or yellow colour upon the use of large excesses of $LiAlH_4$. This resulted in a significant decrease in yield of the desired diphenyltin dihydride. Thus, in order to elucidate the nature of possible over-reaction products, analytically pure Ph_2SnH_2 was reacted with $LiAlH_4$.[22]

In an initial reaction, an equimolar mixture of the two reagents in THF was observed to provide a persistent bubbling and the formation of a dark red solution, as well as a flocculent white precipitate, identified as AlH_3 by IR spectroscopy. Addition of 12-crown-4 (hereafter, 12-Cr-4) and storage at −30 °C yielded a small amount of an intensely yellow material that was thought to be a single, crystalline product. X-ray diffraction analysis, however, indicated this material to be a disordered mixture of two oligostannane dianions (**1** and **2**). In order to access analytically

[a] *6330 Institute of Inorganic Chemistry, Graz University of Technology, Stremayrgasse 9/V, Austria. E-mail: roland.fischer@tugraz.at*
[b] *Department of Chemistry, University of Bath, Claverton Down, Bath BA2 7AY, UK. E-mail: D.J.Liptrot@bath.ac.uk*

† Electronic supplementary information (ESI) available: Synthetic procedures, spectroscopic data, refinement details for single crystal X-ray crystallography. CCDC 1561478–1561482. For ESI and crystallographic data in CIF or other electronic format see DOI: 10.1039/c9cc07976a

pure samples of **1** and **2**, the ratio of $LiAlH_4$ to Ph_2SnH_2 was optimised.

The reaction of 7 equivalents of diphenyltin dihydride with two equivalent of $LiAlH_4$ in THF or DME gave access to crystalline, analytically pure $[Ph_{10}Sn_7]^{2-}[Li(12\text{-}Cr\text{-}4)_2]^+_2$, **1**, in moderate yields after the addition of 12-Cr-4 and storage at −30 °C. Similarly, $[Ph_{12}Sn_8]^{2-}[Li(12\text{-}Cr\text{-}4)_2]^+_2$, **2**, was obtained by applying analogous conditions albeit with a 8 : 2 ratio of Ph_2SnH_2 : $LiAlH_4$. These optimised conditions yielded material suitable for X-ray crystallography as orange and red crystals, respectively. Higher tin to alumane ratios of 8 : 1 and above yielded the bicyclo[2.2.2]heptastanna-1-ide $[Ph_{13}Sn_8]^-[Li(12\text{-}Cr\text{-}4)_2]^+$, **3**. **3** was characterised by NMR and UV-vis spectroscopy as well as X-ray crystallography.[23] A Ph_2SnH_2 : $LiAlH_4$ ratio of 1 : 0.75 and 1 : 2 led to the formation of elemental tin and compounds **4** and **5** which contain discrete $[PhAlH_3]^-$ and $[Ph_3AlH]^-$ anions and charge separated $[Li{\cdot}(12\text{-}Cr\text{-}4)_2]^+$ or $[Li{\cdot}(DME)(12\text{-}Cr\text{-}4)]^+$ counterions. The formation of **4** and **5** demonstrates net phenyl group transfer from tin to aluminium which provides the tertiary tin bridgeheads in **1–3** with less than the original two phenyl groups per tin. NMR spectroscopic interrogation of the reaction mixtures indicated the initial formation of benzene and of the anion $[HPh_2Sn]^-$ (^{119}Sn: −180.5 ppm, $^1J_{^1H-^{119}Sn}$ = 152 Hz),[20] which undergoes subsequent dehydrogenative coupling with excess Ph_2SnH_2 to cause the intermediate formation of various unidentified oligostannyl anions. Isotopic labelling experiments showed the predominant formation of H_2 in the reaction of Ph_2SnH_2 with $LiAlD_4$, while treatment of Ph_2SnD_2 with $LiAlH_4$ gave D_2 (see ESI† page S31).

1 and **2** constitute the first reports of a bicyclo[2.2.1]-heptastannane-1,4-diide and bicyclo[2.2.2]octastannane-1,4-diide, respectively, and both crystallise in the presence of 2 $[Li{\cdot}(12\text{-}Cr\text{-}4)_2]^+$ counterions as charge separated structures. In the solid state structure of the bicyclo[2.2.1]heptastannane-1,4-diide **1** (Fig. 1) the anionic bridgeheads Sn1 and Sn7 are separated by an intramolecular distance of 5.04 Å. The angles around Sn1 and Sn7 sum to 265.8° (Sn1) and 264.6° (Sn7), suggesting high p-orbital contribution in bonding orbitals at Sn1 and Sn7 and implying significant s-orbital character for the lone pair at these anionic tin atoms.

The bicyclo[2.2.2]octastanna-1,4-diide **2** (Fig. 1), features a less constrained geometry in the solid state with angles around the bridgehead atoms Sn1 and Sn8 just above 90° (sum of angles around Sn1 = 276.05° and Sn8 = 274.08°). The monoanion **3** displays two distinctly different environments for the bridgehead tin atoms with a highly pyramidalised anionic tin atom Sn1 (sum of angles 287.69°) and a more tetrahedral geometry at the phenyl substituted, formally neutral bridgehead Sn4 (sum of Sn–Sn–Sn angles 318.62°). The bridgehead atoms, Sn1 and Sn4, are separated by 5.27 Å in **3**, which is *ca.* 0.67 Å less than in **2**. In contrast to **1**, compounds **2** and **3** are both twisted in the solid state (see ESI† Fig. S2.2, page S-7 and S2.3, page S-8). Compounds **4** and **5** (Fig. 1) containing discrete $[PhAlH_3]^-$ and $[Ph_3AlH]^-$ anions and charge separated $[Li{\cdot}(12\text{-}Cr\text{-}4)_2]^+$ or $[Li{\cdot}(DME)(12\text{-}Cr\text{-}4)]^+$ counterions, respectively, display tetrahedral aluminium atoms with Al–C distances slightly greater than 2.0 Å.

The ^{119}Sn{^{1}H} NMR spectra of **1**, **2** and **3** indicate that these cages persist in solution, as evidenced by chemical shifts and the observed ^{119}Sn/^{117}Sn couplings (Fig. 2, ESI† Section 4 pages S-14–S-26). **1** displays three resonances at 200.3 ($Ph_2\mathit{Sn}$), 35.7 ($Ph_2\mathit{SnSn}Ph_2$) and −857.3 (Sn^-) ppm for which the coupling pattern is in full agreement with the bicyclo[2.2.1]heptastanna–1,3–diide framework in solution. $^1J_{^{119}Sn-^{119/117}Sn}$ coupling constants originating from the anionic bridgehead atoms are large with values of 4640/4430 Hz for the interaction with the monotin–bridge. In the case of coupling between the bridgehead tin atoms and the ditin bridges, values of 5990/5710 Hz for the $^1J_{^{119}Sn-^{119/117}Sn}$ coupling and 1130/1080 Hz for the $^2J_{^{119}Sn-^{119/117}Sn}$ coupling are observed. The relatively large ^1J values compare to a smaller $^1J_{^{119}Sn-^{117}Sn}$ coupling constant of 3940 Hz for chemically equivalent tin atoms within the same ditin bridge.

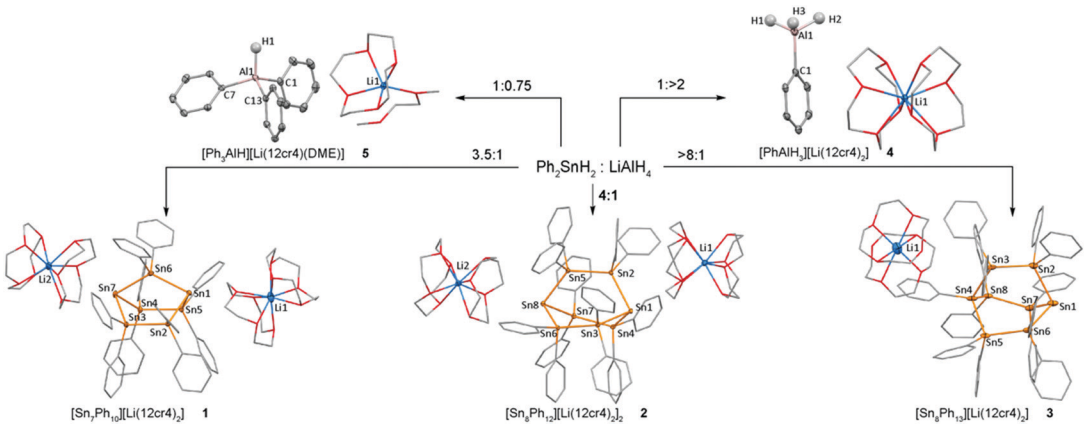

Fig. 1 Formation of anionic oligotin cages **1–3** and phenyl aluminium hydrides **4** and **5**. Metal atoms are drawn at 30% probability level, only hydrogen atoms attached to Al are shown, all other H atoms are omitted for clarity. For full geometric parameters, see ESI† pages S-7–S-9. Selected bond angles (°) **1**: Sn2–Sn1–Sn5 94.37(2); Sn2–Sn1–Sn6 86.75(1); Sn5–Sn1–Sn6 84.67(1); Sn3–Sn7–Sn4 93.52(2); Sn3–Sn7–Sn6 85.41(1); Sn4–Sn7–Sn6 85.69(1). **2**: Sn2–Sn1–Sn3 91.29(2); Sn2–Sn1–Sn4 91.41(2); Sn3–Sn1–Sn4 93.35(2); Sn5–Sn8–Sn6 90.95(2); Sn5–Sn8–Sn7 89.00(2); Sn6–Sn8–Sn7 94.13(2). **3**: Sn2–Sn1–Sn6 96.92(8); Sn2–Sn1–Sn7 95.47(8); Sn6–Sn1–Sn7 95.30(8); Sn3–Sn4–Sn5 106.93(8); Sn3–Sn4–Sn8 105.22(8); Sn5–Sn4–Sn8 106.47(8).

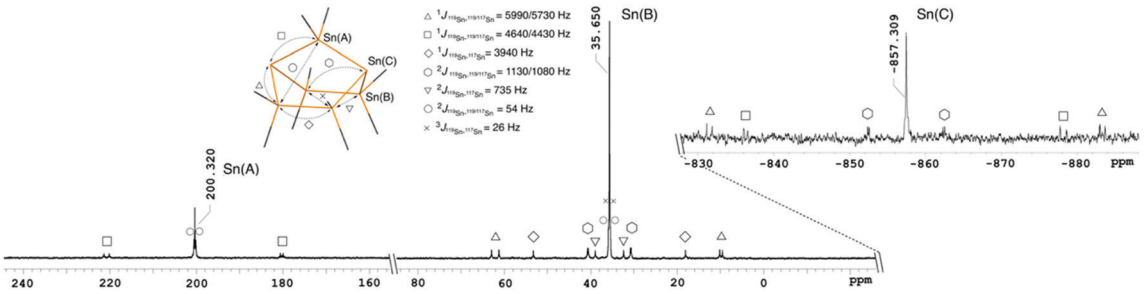

Fig. 2 $^{119}Sn\{^1H\}$ NMR spectrum of **1** in d_3-acetonitrile showing Sn–Sn couplings indicative of the solution integrity of these compounds.

ng to its higher molecular symmetry, only two resonances are observed in the $^{119}Sn\{^1H\}$ NMR spectrum of **2**, with peaks at −316.8 ($Ph_2SnSnPh_2$) and −585.0 (Sn^-) ppm. The ^1J and the $^2J_{^{119}Sn-^{119/117}Sn}$ coupling constants between the bridgehead tin atoms and the $Ph_2SnSnPh_2$ bridges are 5020/4800 Hz and 807/770 Hz, respectively. Again, a smaller $^1J_{^{119}Sn-^{117}Sn}$ coupling constant of 3610 Hz is observed for neighbouring diphenyltin fragments. The monoanion **3** displays four distinct signals in the $^{119}Sn\{^1H\}$ NMR spectrum at −183.1 ($Ph_2\mathit{Sn}Sn^-$), −238.6 ($Ph_2\mathit{Sn}SnPh$), −470.8 ($\mathit{Sn}Ph$) and −757.9 (Sn^-) ppm. Notably, the coupling constant of the tricoordinate, anionic tin atom in **3** is larger ($^1J_{^{119}Sn-^{119/117}Sn}$ = 6410/6090 Hz) in comparison to the signal of the neutral tin bridgehead, which is only 1150/1090 Hz.

Experimentally observed NMR chemical shifts were replicated by DFT calculations. To support the bonding model proposed based on the structural analysis of **1–3**, the anions in these compounds were interrogated by DFT calculations employing different methods and basis sets. (For computational details and references see ESI† page S-84). The highest occupied molecular orbitals of **1–3** are shown in Fig. 3. These orbitals are in each case associated with the lone pairs on the anionic bridgehead tin atom(s) with contribution of the tin skeleton and show significant s-character.

This supports the conclusion of significant p-orbital involvement in the Sn–Sn bonding of the bridgehead tin atoms inferred from their experimental solid state structures. The frontier orbitals of **1–3** (Fig. 3 and ESI† pages S-37–S-40) display distinct groupings into sets of orbitals with σ-, σ*- and π*-character interpreted as the onset of band-like behaviour. The HOMO to HOMO−8 ($\Delta E_{HOMO-HOMO-8}$ = 1.78 eV) for **2** and HOMO to HOMO−7 orbitals for **1** ($\Delta E_{HOMO-HOMO-7}$ = 2.03 eV) and **3** ($\Delta E_{HOMO-HOMO-7}$ = 1.66 eV) essentially represent the σ-bonded tin cores with only minor orbital contributions from the phenyl substituents. Within HOMO–LUMO energy gaps of only 2.33 eV (**1**), 2.15 eV (**2**) and 2.47 eV (**3**), the character of the frontier orbitals changes to phenyl based π* character.

The LUMO to LUMO+n orbitals (n = 20 in **1**, n = 23 in **2**, n = 25 in **3**) are similar in orbital energy and all localised on the phenyl substituents. This manifold of π* orbitals is then followed by a set of orbitals with predominant σ* character of the tin framework, which span energy ranges of 0.78 eV (**1**), 0.81 eV (**2**) and 1.34 eV (**3**). These closely spaced MOs are reflected in the electronic absorptions displayed by **1–3**. The UV-visible spectra of these species do not display distinct absorption maxima and are instead broad and tailing, suggestive of weak but extensive absorptions. Nevertheless, the visibly observed colours for crystals of **1** (orange-yellow), **2** (orange-red) and **3** (bright yellow) are consistent with the expected effects of cage size and charge upon σ-delocalisation[24] inferred from the DFT calculations.

In summary, the reaction of Ph_2SnH_2 with $LiAlH_4$ provides facile access to the charge-separated species, **1**, **2** and **3**, comprising an unprecedented set of structural motifs in anionic oligostannane cages. **1** and **2** constitute new dianionic covalent tin cages and we propose that they will provide convenient synthons in further transformations because of their charged nature and solution integrity. The electronic structure of **1–3** was interrogated computationally and support the presence of σ-delocalisation.

We wish to acknowledge the European COST Network for Smart Inorganic Polymers for providing funding to allow collaboration on this work. B. G. Steller gratefully acknowledges the Austrian Academy of Sciences for supporting this work with the DOC Fellowship. We thank the EPSRC (UK) for the support of a DTP studentship for A. S. S. Wilson and grant EP/R020752/1. Some DFT calculations were carried out using the Balena High Performance Computing (HPC) Service at the University of Bath.

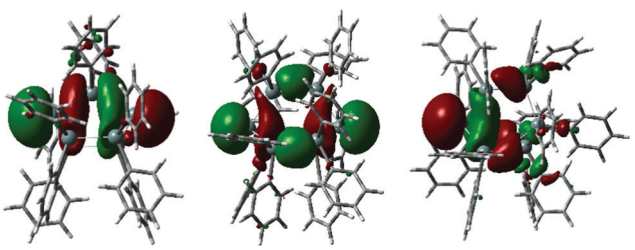

Fig. 3 Highest occupied molecular orbitals of **1–3**, for full computational details see ESI† Section 5, pages S-34–S-83.

Conflicts of interest

The authors declare no conflict of interest.

Notes and references

1 (*a*) S. C. Sevov and J. M. Goicoechea, *Organometallics*, 2006, **25**, 5678–5692; (*b*) T. F. Fässler, *Coord. Chem. Rev.*, 2001, **215**, 347–377.
2 (*a*) A. Schnepf, *Chem. Soc. Rev.*, 2007, **36**, 745–758; (*b*) A. Schnepf, *Struct. Bonding*, 2016, 193–223.

3 (*a*) F. S. Kocak, D. O. Downing, P. Zavalij, Y. F. Lam, A. N. Vedernikov and B. Eichhorn, *J. Am. Chem. Soc.*, 2012, **134**, 9733–9740; (*b*) F. S. Kocak, P. Y. Zavalij, Y.-F. Lam and B. W. Eichhorn, *Chem. Commun.*, 2009, 4197–4199; (*c*) F. S. Kocak, D. O. Downing, P. Zavalij, Y. F. Lam, A. N. Vedernikov and B. Eichhorn, *J. Am. Chem. Soc.*, 2012, **134**, 9733–9740; (*d*) D. J. Chapman and S. C. Sevov, *Inorg. Chem.*, 2008, **47**, 6009–6013; (*e*) C. B. Benda, M. Waibel and T. F. Fässler, *Angew. Chem., Int. Ed.*, 2015, **54**, 522–526.
4 (*a*) C. Schrenk, A. Kubas, K. Fink and A. Schnepf, *Angew. Chem., Int. Ed.*, 2011, **50**, 7273–7277; (*b*) C. Schrenk, I. Schellenberg, R. Pöttgen and A. Schnepf, *Dalton Trans.*, 2010, **39**, 1872–1876; (*c*) C. Schrenk and A. Schnepf, *Chem. Commun.*, 2010, **46**, 6756–6758.
5 (*a*) C. Schrenk, J. Helmlinger and A. Schnepf, *Z. Anorg. Allg. Chem.*, 2012, **638**, 589–593; (*b*) C. Schrenk, B. Gerke, R. Pöttgen, A. Clayborne and A. Schnepf, *Chem. – Eur. J.*, 2015, **21**, 8222–8228.
6 C. Schrenk, F. Winter, R. Pöttgen and A. Schnepf, *Inorg. Chem.*, 2012, **51**, 8583–8588.
7 C. Schrenk, F. Winter, R. Pöttgen and A. Schnepf, *Chem. – Eur. J.*, 2015, **21**, 2992–2997.
8 J.-J. Maudrich, C. P. Sindlinger, F. S. W. Aicher, K. Eichele, H. Schubert and L. Wesemann, *Chem. – Eur. J.*, 2017, **23**, 2192–2200.
9 (*a*) E. Rivard, J. Steiner, J. C. Fettinger, J. R. Giuliani, M. P. Augustine and P. P. Power, *Chem. Commun.*, 2007, 4919–4921; (*b*) G. Prabusankar, A. Kempter, C. Gemel, M. K. Schröter and R. A. Fischer, *Angew. Chem., Int. Ed.*, 2008, **47**, 7234–7237; (*c*) B. E. Eichler and P. P. Power, *Angew. Chem., Int. Ed.*, 2001, **40**, 796–797; (*d*) A. F. Richards, B. E. Eichler, M. Brynda, M. M. Olmstead and P. P. Power, *Angew. Chem., Int. Ed.*, 2005, **44**, 2546–2549; (*e*) J. Wiederkehr, C. Wölper and S. Schulz, *Chem. Commun.*, 2016, **52**, 12282–12285; (*f*) M. Brynda, R. Herber, P. B. Hitchcock, M. F. Lappert, I. Nowik, P. P. Power, A. V. Protchenko, A. Růžička and J. Steiner, *Angew. Chem., Int. Ed.*, 2006, **45**, 4333–4337; (*g*) C. P. Sindlinger, A. Stasch, H. F. Bettinger and L. Wesemann, *Chem. Sci.*, 2015, **6**, 4737–4751; (*h*) C. P. Sindlinger, W. Grahneis, F. S. W. Aicher and L. Wesemann, *Chem. – Eur. J.*, 2016, **22**, 7554–7566; (*i*) C. P. Sindlinger, F. S. W. Aicher, H. Schubert and L. Wesemann, *Angew. Chem., Int. Ed.*, 2017, **56**, 2198–2202; (*j*) L. R. Sita, *Acc. Chem. Res.*, 1994, **27**, 191–197.
10 (*a*) A. Schnepf and H. Schnöckel, *Angew. Chem., Int. Ed.*, 2002, **41**, 3532–3554; (*b*) A. Schnepf and H. Schnöckel, Nanostructural Element Modifications: Synthesis and Structure of Elementoid Gallium Clusters, in *ACS Symposium Series 822, Group 13 Chemistry*, ed. P. J. Shapiro and D. A. Atwood, American Chemical Society, Washington DC, 2002.
11 (*a*) L. R. Sita and R. D. Bickerstaff, *J. Am. Chem. Soc.*, 1989, **111**, 6454–6456; (*b*) C. Drost, M. Hildebrand and P. Lönnecke, *Main Group Met. Chem.*, 2002, **25**, 93–98.
12 L. R. Sita and I. Kinoshita, *J. Am. Chem. Soc.*, 1992, **114**, 7024–7029.
13 C. P. Sindlinger and L. Wesemann, *Chem. Sci.*, 2014, **5**, 2739–2746.
14 (*a*) L. R. Sita and I. Kinoshita, *J. Am. Chem. Soc.*, 1991, **113**, 5070–5072; (*b*) L. R. Sita and I. Kinoshita, *J. Am. Chem. Soc.*, 1990, **112**, 8839–8843; (*c*) D. Nied, E. Matern, H. Berberich, M. Neumaier and F. Breher, *Organometallics*, 2010, **19**, 6018–6037; (*d*) P. Vasko, S. Wang, H. M. Tuononen and P. P. Power, *Angew. Chem., Int. Ed.*, 2015, **54**, 3802–3805; (*e*) D. Nied and F. Breher, *Chem. Soc. Rev.*, 2011, **40**, 3455–3466.
15 C. Marschner and J. Hlina, Catenated Compounds – Group 14 (Ge, Sn, Pb), in *Comprehensive Inorganic Chemistry II*, ed. J. Reedijk and K. Poeppelmeier, Elsevier, Oxford, 2013, vol. 1.
16 (*a*) S. Masamune and L. R. Sita, *J. Am. Chem. Soc.*, 1985, **107**, 6390–6391; (*b*) L. R. Sita and I. Kinoshita, *J. Am. Chem. Soc.*, 1991, **113**, 1856–1857; (*c*) N. Wiberg, H.-W. Lerner, H. Nöth and W. Ponikwar, *Angew. Chem., Int. Ed.*, 1999, **38**, 1103–1105.
17 (*a*) L. R. Sita and I. Kinoshita, *Organometallics*, 1990, **9**, 2865–2867; (*b*) N. Wiberg, H. W. Lerner, S. Wagner, H. Nöth and T. Seifert, *Z. Naturforsch. B*, 1999, **54**, 877–880.
18 M. Wagner, M. Lutter, B. Zobel, W. Hiller, M. H. Prosenc and K. Jurkschat, *Chem. Commun.*, 2015, **51**, 153–156.
19 (*a*) T. Imori, V. Lu, H. Cai and T. D. Tilley, *J. Am. Chem. Soc.*, 1995, **117**, 9931–9940; (*b*) P. Braunstein, J. Durand, X. Morise, A. Tiripicchio and F. Ugozzoli, *Organometallics*, 2000, **19**, 444–450; (*c*) P. Braunstein and X. Morise, *Chem. Rev.*, 2000, **100**, 3541–3552; (*d*) N. R. Neale and T. D. Tilley, *J. Am. Chem. Soc.*, 2002, **124**, 3802–3803; (*e*) F. Choffat, P. Smith and W. Caseri, *J. Mater. Chem.*, 2005, **15**, 1789–1792; (*f*) F. Choffat, S. Käser, P. Wolfer, D. Schmid, R. Mezzenga, P. Smith and W. Caseri, *Macromolecules*, 2007, **40**, 7878–7889.
20 M. Trummer and W. Caseri, *Organometallics*, 2010, **29**, 3862–3867.
21 (*a*) A. E. Finholt, A. C. Bond, Jr., K. E. Wilzbach and H. I. Schlesinger, *J. Am. Chem. Soc.*, 1947, **69**, 2692–2696; (*b*) N. Braia, Y. Saihi, A. E. Azzouzi and F. Ferkous, *Asian J. Chem.*, 2009, **21**, 4628–4634.
22 The use of analytically pure $LiAlH_4$ (recryst. from diethyl ether) is crucial for the successful control of the stoichiometry.
23 The anionic part in **3** was well resolved and is fully consistent with NMR data. The X–ray structure determination of the cationic part and residual solvent molecules, however, was hampered by twinning and disorder. See ESI† pages S-4 and S-5.
24 (*a*) M. S. Hill, Homocatenation of Metal and Metalloid Main Group Elements, in *Metal-Metal Bonding: Structure and Bonding*, ed. G. Parkin, Springer, Berlin, 2010, vol. 136; (*b*) M. Jovanovic, D. Antic, D. Rooklin, A. Bande and J. Michl, *Chem. – Asian J.*, 2017, **12**, 1250–1263; (*c*) M. Jovanovic and J. Michl, *J. Am. Chem. Soc.*, 2018, **140**, 11158–11160; (*d*) M. Jovanovic and J. Michl, *J. Am. Chem. Soc.*, 2019, **141**, 13101–13113.